

Design And Simulation Of A Maximum Power Point Tracking (Mppt) For A Boost Converter Fed From A Pv Source

Ifeanyi B. Ezugwu¹, J.U. Agber², Nentawe Y. Goshwe³

¹(Computer Engineering Technology department, Dorben Polytechnic, Bwari, Nigeria)

^{2,3}(Electrical and Electronics Engineering department, University of Agriculture, Makurdi, Nigeria)

Corresponding Author: Ifeanyi B. Ezugwu

ABSTRACT: The constant variations in sun's irradiation and operating temperature of solar cells are the inherent issues with energy generation through photovoltaic (PV) source. Changes in irradiance significantly affects the PV output current, but have a much smaller effect on voltage while changes in temperature slightly affects the output current but significantly changes the voltage which decreases with increases in cell temperature, resulting in losses and a net reduction in power and efficiency. This constant change in irradiation and temperature causes a shift in the I-V characteristic curve known as Maximum Power Point (MPP) where PV system gives highest efficiency and produces highest output power which it transfers to the load. The main source of the power loss is the failure to track MPP. So, Maximum Power Point Tracking (MPPT) is essential to operate PV system at MPP. The perturb and observe (P&O) MPPT control mechanism controls the duty cycle of the boost converter to ensure that the maximum possible power of the PV module is extracted at varying perturbations, irradiance, and temperature. The MPPT controller is interfaced to a hard and soft switching boost converter and their performance was observed. The P&O algorithms and the entire system are modeled in MATLAB/Simulink. The results obtained show that at irradiation of 600W/m² and 1000W/m², the MPPT hard switching boost converter generates 2.774kW and 2.895kW power respectively at a constant temperature of 25 degrees Celsius and at irradiation of 600 W/m² and 1000 W/m², the MPPT soft switching boost converter generates 11.117kW and 11.585kW power respectively at a constant temperature of 25 degrees Celsius. This shows that soft switching technique reduces switching losses and generates higher output power compared to the hard switching method. It can also be seen from the results that MPPT control can eliminate the constant deviations in maximum operating power of the PV module which results to reduction of energy losses and increase in efficiency.

KEYWORDS –Boost converter, CCM, Perturb and observe, Photovoltaic, Maximum Power Point Tracking.

Date of Submission: 03-08-2018

Date of acceptance: 17-09-2018

I. INTRODUCTION

Photovoltaics are semiconductor materials which convert solar irradiation in the visible spectrum to generate direct current (DC)[1]. When sunlight is absorbed by these materials, the solar energy knocks electrons loose from their atoms, allowing the electrons to flow through the material to produce electricity[2]. This process of converting light (photons) to electricity (voltage) is what is actually referred to as photovoltaic (PV) effect.

The performance of a solar cell is measured in terms of its efficiency at turning sun irradiation into electricity. Only sunlight of certain energies will work efficiently to create electricity, and much of it is reflected or absorbed by the materials that make up the cell. As a result, a typical commercial solar cell has a considerably very low efficiency. Low efficiency means that plenty arrays are needed, and that implies increased cost. Several research works has been carried out to propound the best methods for improving solar cell efficiencies and a lot of success has been recorded.

Sequel to this, the major focus of this paper is to show further, the improvements in solar power generation through the use of a maximum power point tracker (MPPT) in addition with a switching boost converter. Also the efficiency and effectiveness of the hard and soft boost converter power circuits with an MPPT is compared. A MPPT is used for extracting the maximum power from the solar PV module and transferring that power to the load [3] [4]. The key to extracting the most power from the panels is to maintain an

output impedance such that the solar panels operate at a point that equals its maximum power point (MPP). The MPP is the operating point required to optimize the output power of the panels[5]. In order to increase the efficiency of the solar array, a switching boost converter is interfaced to extract the most power and also control the voltage of the solar array by varying the duty cycle of the boost converter. Varying the duty cycle enables the voltage and current to provide the highest power at a specific voltage level. In order to reach this voltage level, a control algorithm is implemented to track and follow the highest input power from the solar array. When this algorithm is functioning correctly, it is said to be an MPPT.

II. SYSTEMS ANALYSIS

The studied system comprises three essential components, as illustrated in Figure 1. A DC-DC switching boost converter along with a MPPT controller to operate the PV system in such a way it can transfer maximum capable power to the load. Here, the inputs of the boost converter are fed from voltage and current of the PV terminals, while the output of the MPPT P&O technique provides its duty cycle.

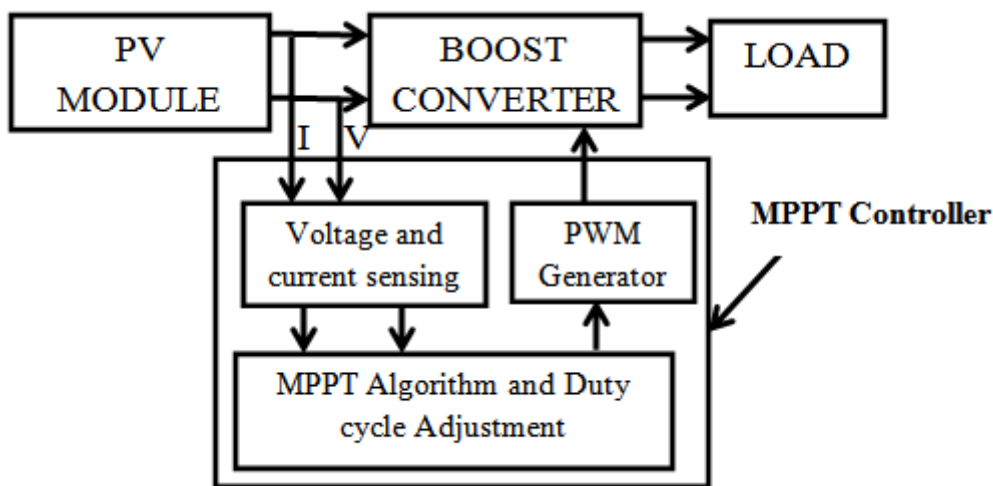


Figure 1: System block diagram

1. Modeling of Solar PV array

The mathematical representation of single and double diode models of a PV cell is as shown below:

1.1 Single Diode Model

The characteristic equations for a single diode model is expressed as follows,

$$I_{pv} = I_{PH} - I_s \left[e^{\frac{q(V_{pv} + I + R_s)}{KT_c A}} - 1 \right] - \frac{(V_{pv} + I + R_s)}{R_{SH}} \tag{1}$$

Where $I_{pv} = 1 - \frac{A1}{A2}$ 2

$$A1 = I_{PH} - 1 - I_s \left[e^{\frac{q(V_{pv} + I + R_s)}{KT_c A}} - 1 \right] \tag{3}$$

$$A2 = -1 - I_s \left[e^{\frac{q(V_{pv} + I + R_s)}{KT_c A}} - 1 \right] \left[\frac{q(R_s)}{kT_c A} \right] \tag{4}$$

$$I_{PH} = [I_{SC} + k_i(T_c - T_{ref})]G \tag{5}$$

$$I_s = I_{RS} \left(\frac{T_c}{T_{ref}} \right)^{3/A} \left[e^{\frac{qEG \left(\frac{1}{T_{ref}} - \frac{1}{T_c} \right)}{KA}} \right] \tag{6}$$

$$I_R = \frac{I_{SC}}{\left[\frac{qV_0 C}{e^{KAN_s T_c}} - 1 \right]} \tag{7}$$

Where,

A: Ideality factor

N_s: Number of cells in series

q: Electron Charge, = 1.6×10⁻²³ C;

K: Boltzmann’s constant, = 1.38 × 10⁻¹⁹ J/K;

ΔT: Temperature variance between STC and maximum expected temperature

Usually, the data sheet of PV module or array provides some of the PV parameters such as open circuit voltage, short circuit current, temperature coefficient and others based on the Standard Test Condition (STD), which are 1000 W/m² irradiation and 25 degree Celsius of temperature.

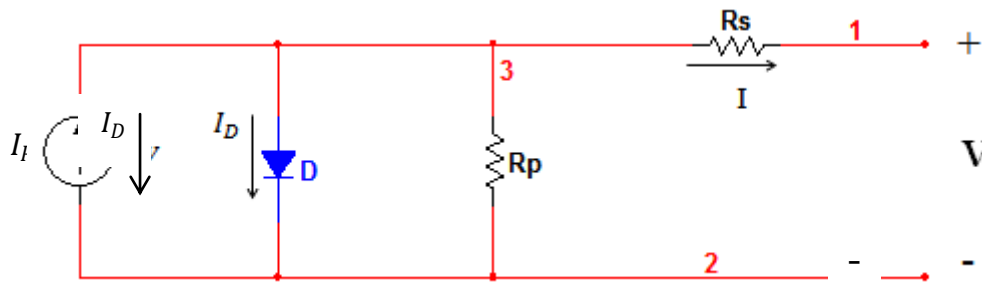


Figure2: Single diode model PV cell

The load current equation is given by

$$I = I_{PV} - I_0 \left[\exp\left(\frac{V+IR_s}{aV_T}\right) - 1 \right] - \frac{(V+IR_s)}{R_p} \tag{8}$$

In above equation I_{PV} represents photo current and I_0 is reverse saturation current which are given by (9) and (10).

$$I_{PV} = (I_{PV_STC} + K_1\Delta T) \frac{G}{G_{STC}} \tag{9}$$

$$I_D = I_{0_STC} \left(\frac{T_{STC}}{T}\right)^3 \exp\left[\frac{qE_g}{ak} \left(\frac{1}{T_{STC}} - \frac{1}{T}\right)\right] \tag{10}$$

1.1.2 Double Diode Model

The single diode model neglects the recombination losses in depletion region. In actual practice these recombination losses causes a substantial loss, especially low voltages. To consider losses more precise two-diode model is required[6] as is shown in Figure 3.

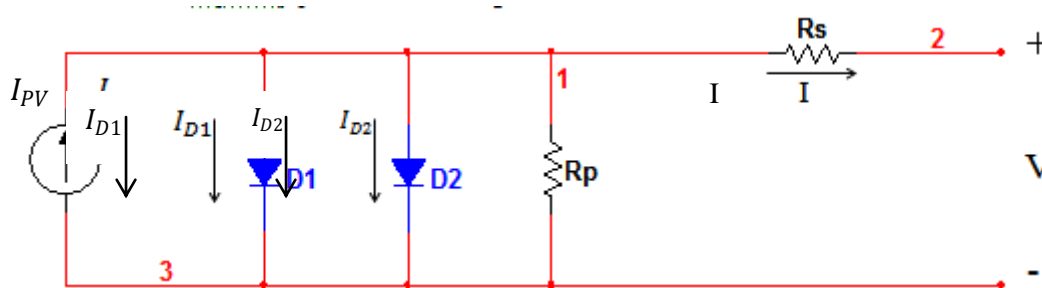


Figure 3: Two diode model PV cell

The equations for single diode model can be modified to obtain current expression for double diode model as follows.

$$I = I_{PV} - I_{01} \left[\exp\left(\frac{V+IR_s}{a_1V_T}\right) - 1 \right] - I_{02} \left[\exp\left(\frac{V+IR_s}{a_2V_T}\right) - 1 \right] - \frac{(V+IR_s)}{R_p} \tag{11}$$

Where

$$I_{d1} = I_{01} \left[\exp\left(\frac{V+IR_s}{a_1V_T}\right) - 1 \right] \tag{12}$$

$$I_{d2} = I_{02} \left[\exp\left(\frac{V+IR_s}{a_2V_T}\right) - 1 \right] \tag{13}$$

$$I_{PV} = (I_{PV_STC} + K_1\Delta T) \frac{G}{G_{STC}} \tag{14}$$

$$I_{01} = I_{02} = \frac{I_{SC_STC} + K_1\Delta T}{\exp\left[\frac{(V_{OC_STC} + K_V\Delta T)}{\left(\frac{a_1+a_2}{p}\right)V_T}\right] - 1} \tag{15}$$

1.2 Boost converter design

A boost converter can be defined as an inductor, which is first switched in parallel to a voltage source, which is then abruptly disconnected forcing the buildup of a flyback voltage across the inductor that is then added to the input voltage to obtain an output voltage always bigger than the input voltage. Figure 4 is a schematic of an

ideal boost converter. The components of this converter are ideal and it is assumed that it operates in continuous conduction mode (CCM).

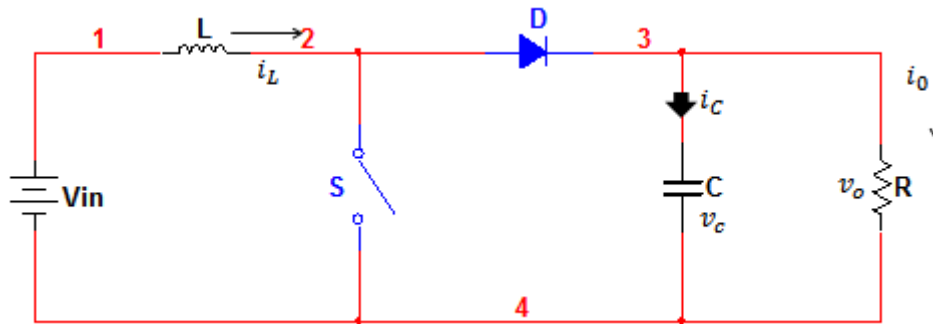


Figure 4: Circuit diagram of a boost converter.

1.2.1 Ideal Boost converter Operating stages

ON state

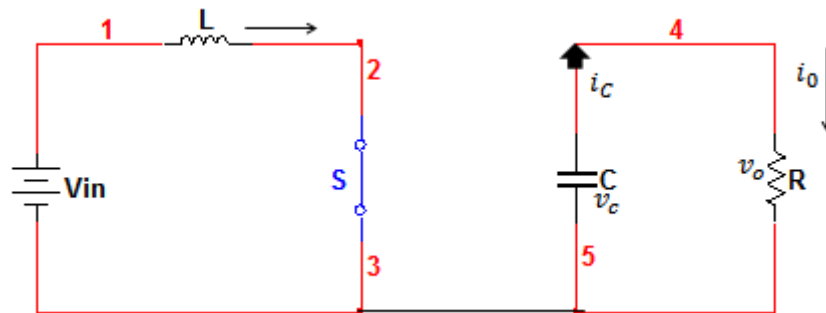


Figure 5: Boost converter ON state

At this stage, the switch S is ON

$$L \frac{di_L}{dt} = v_{in} \tag{20}$$

$$C \frac{dv_0}{dt} = -\frac{v_0}{R} \tag{21}$$

OFF state

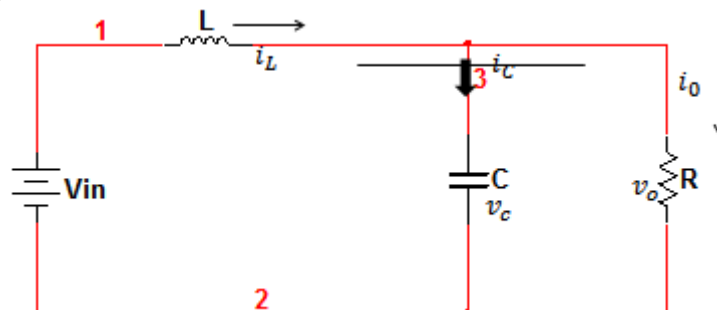


Figure 6: Boost converter off state

At this stage, the switch S is off

$$L \frac{di_L}{dt} = v_{in} - v_0 \tag{16}$$

$$C \frac{dv_0}{dt} = i_L - \frac{v_0}{R} \tag{17}$$

Therefore a boost converter output voltage is generated by the switch opening and closing at a frequency of 1/T where T is the switch cycle period. The ratio of the on-time to the switch cycle period is referred to as the duty cycle (D).

$$D = \frac{t_{ON}}{T} \tag{18}$$

$$T = t_{ON} + t_{OFF} \quad 19$$

Therefore, averaging state equations over a switching cycle implies:

$$L \frac{di_L}{dt} = v_{in} - (1-d)v_0 \quad 20$$

$$C \frac{dv_0}{dt} = (1-d)i_L - \frac{v_0}{R} \quad 21$$

1.2.2 Boost converter components selection

Parameters required for the power stage of a boost converter

the input voltage range: $V_{in\ min} = 0V$, and $V_{in\ max} = 82.6V$; maximum resistive load: = 75 ohm ; Switch frequency of the converter: $f = 40\text{ kHz}$; Estimated input current ripple: = 9%; Estimated output voltage ripple: = 0.24%; The frequency (f) is chosen to be 40 kHz ; Assuming efficiency (η) of the converter is 90%; $T = \frac{1}{f}$, thus the time period of one cycle switching is (T) = 25 μ sect, t_{on} is the time when the switch is on, f is the frequency, D is the duty cycle, t_{off} is the time when the switch is off, T is the total time period of one cycle of switching.

$$T = t_{on} + t_{off}$$

$$t_{on} = DT$$

$$V_{out} = \frac{V_{PV-MAX}}{1-D}$$

Due to the assumption that the efficiency is 90%, the output power is approximately equal to the input power and the output voltage of the converter under PV panel with $G=1000\text{ W/m}^2$ is:

$$P_{out} = \frac{v_{out}^2}{R_{Load}}$$

$$V_{out} = \sqrt{420 \times 96} \cong 201\text{ volt}$$

$$i_{out} = \sqrt{\frac{420}{96}} \cong 2.09\text{ Amps}$$

$$D = 1 - \frac{P_{pv-max}}{V_{out}} = 1 - \frac{82.6}{201} \cong 0.6$$

Thus the duty cycle of this system will be from 0 to ≈ 0.6 with a resistivity of 96 Ω

The requirement of the current ripple system and power losses will determine the inductor selection. When the switch is on, the voltage across the inductor is given by

$$V_L(t) = L \frac{di(t)}{dt} = V_{in}$$

$$\frac{di(t)}{dt} = \frac{V_L(t)}{L} = \frac{V_{in}}{L}$$

The inductor current increases with a constant slope $\frac{V_{in}}{L}$

When the switch is off, the voltage across the inductor is given by

$$V_L(t) = L \frac{di(t)}{dt} = V_{in} - V_{out} - V_d$$

$$\frac{di_L(t)}{dt} = \frac{V_L(t)}{L} = \frac{V_{in} - V_{out} - V_d}{L}$$

V_d is the voltage across the diode

The change in the inductor current during one cycle is:

$$2\Delta i_L = \frac{V_{in}}{L} t_{on} + \frac{V_{in} - V_{out} - V_d}{L} t_{off} \quad 22$$

The inductor current ripple

$$\Delta i_{Lp} = 9\% i_L = 5.08 \times \frac{9}{100} = 0.4572\text{ A}$$

The above value for inductor ripple current can also be obtained from (23) below

$$\Delta i_L = \frac{V_{in} \times D}{f_s \times L} \quad 23$$

The peak- to - peak current $\Delta i_{Lp-p} = 2\Delta i_L = 0.9144\text{ A}$

To select the most suitable inductor, below can be applied:

$$L = \frac{V_{in} \times DT}{\Delta i_{Lp-p}} \quad 24$$

$$L = \frac{82.6}{0.9144 \times 40000} \times 0.6 = 1.3549 \times 10^{-3} \cong 1.4\text{mH}$$

Furthermore, taking $\Delta i = 4\%$

$$\Delta i_{Lp} = 4\% i_L = 5.08 \times \frac{4}{100} = 0.2032 \cong 0.2\text{ A}$$

$$L = \frac{82.6}{2 \times 0.2 \times 40000} \times 0.6 = 3.0975 \times 10^{-3} \cong 3.1\text{mH}$$

Hence, looking at both values of the inductors it is observed that with less value of inductance there is more current ripple. A large value of inductance will reduce the current ripple and discontinuous current mode will be surely avoided. Moreover, using a high value of inductor will lead to a high inductor resistance, large size and high cost. To improve the efficiency of the converter the resistance of the inductor should be sufficiently small.

Output capacitor value selection:

Assuming the equivalent series resistance with capacitor is zero:

$$i_c(t) = C \frac{dV_c}{dt} \quad 25$$

When the switch is on, the capacitor supplies the load current

$$i_c(t) = -\frac{V_{out}(t)}{R} = C \frac{dV_c(t)}{dt}$$

$$\frac{dV_c(t)}{dt} = -\frac{V_{out}(t)}{RC}$$

When the switch is off

$$i_c(t) = i_L - \frac{V_{out}(t)}{R} = C \frac{dV_c(t)}{dt} \quad 26$$

$$\frac{dV_c(t)}{dt} = Ri_L - \frac{V_{out}(t)}{RC}$$

$$\Delta V_c = \frac{V_{out}}{RC} t_{on} \quad 27$$

$$\Delta V_c = 0.24\%, \quad \Delta V_{out} = \frac{0.24}{100} \times 201 = 0.48V$$

This implies that,

$$C = \frac{V_{out}}{2\Delta V_c R} t_{on}$$

$$t_{on} = DT = \frac{D}{f}$$

$$C = \frac{201}{2 \times 0.48 \times 96 \times 40000} \times 0.6 \cong 33\mu F$$

But if $\Delta V_c = 1\%$

$$\Delta V_c = 1\% V_{out} = \frac{201 \times 1\%}{201} = 2.01V$$

$$C = \frac{201}{2 \times 2.01 \times 96 \times 40000} \times 0.6 \cong 9\mu F$$

Hence, it can be observed that with less value of capacitance there is more voltage ripple, a large capacitor will reduce the voltage ripple and help the output stability, however the output voltage will be slow to reach a steady state level.

1.3 Perturb and Observe MPPT Controller Design

The P&O MPPT technique introduces a secondary influence into the system that causes the voltage to deviate slightly. This perturbation causes changes in the power of the solar module. If the power increases due to the perturbation then the perturbation is continued in that direction [7]. After the peak power is reached the power at the next instant decreases and hence after that the perturbation reverses. When the steady state is reached the algorithm oscillates around the peak point. In order to keep the power variation small the perturbation size is kept very small. The algorithm is developed in such a manner that it sets a reference voltage of the module corresponding to the peak voltage of the module. The P&O algorithm as shown below in Fig. 7 and Fig. 8 operates by increasing or decreasing the array terminal voltage, or current, at regular intervals and then comparing the PV output power with that of the previous sample point [8]. If the PV array operating voltage changes and power increases ($dP/dV_{PV} > 0$), the control system adjusts the PV array operating point in that direction; otherwise the operating point is moved in the opposite direction. At each perturbation point, the algorithm continues to operate in the same manner [9]. The perturbation cycle is repeated until it reaches the maximum power at ($\Delta P_{PV} = 0$).

The main advantage of this approach is the simplicity of the technique. Furthermore, previous knowledge of the PV panel characteristics is not required. In its simplest form, this method generally exhibits good performance provided the solar irradiation does not vary too quickly [5]. At steady state, the operating point oscillates around the MPP voltage and usually fluctuates slightly. For this reason, the perturbation frequency should be low enough so that the system can reach steady state before the next perturbation.

$$\frac{dP}{dV} = 0$$

at MPP

28

$\frac{dP}{dV} > 0$ left of MPP 29
 $\frac{dP}{dV} < 0$ right of MPP 30

The algorithm above is illustrated in figure 7 as shown

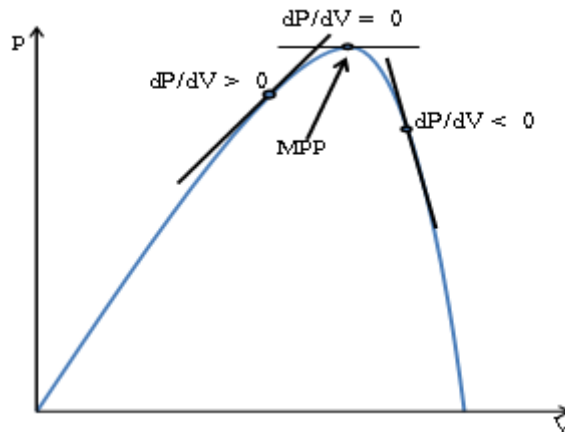


Figure 7: dP/dV at different positions on the power characteristic curve.

1.3.1 Flowchart of the Perturb & Observe method

The figure below is a flow chart of MPPT, perturb and observe algorithm:

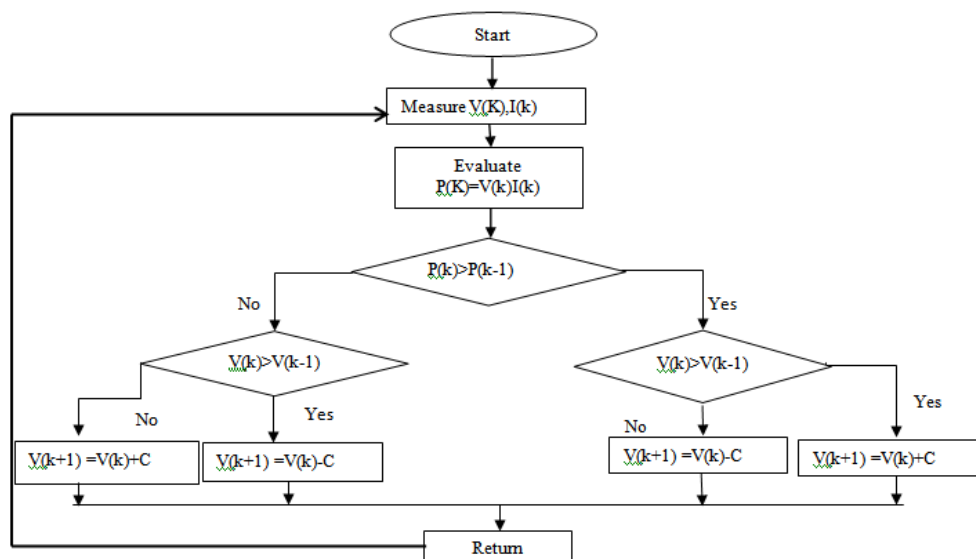


Figure 8: Flowchart of the P&O method

III. SIMULATION AND DISCUSSION

The maximum power point tracking (MPPT) system was simulated with an embedded algorithm in Matlab. The MPPT and the boost converter were interfaced and a PV panel was connected to serve as an input source to the boost converter. The perturb and observe MPPT system as discussed above is meant to introduce perturbation to the PV current at various levels in order to examine the maximum power point of the PV panel. Because of the inefficiency of the panel, a boost converter is used to maximize or increase its efficiency. Hard and soft switching boost converters were interfaced respectively to determine the most effective and efficient power circuit for an MPPT system. Below are the circuit diagrams and various waveforms obtained from simulation in MatlabSimulink.

The various waveforms were obtained by using the plot mechanism in MATLAB.

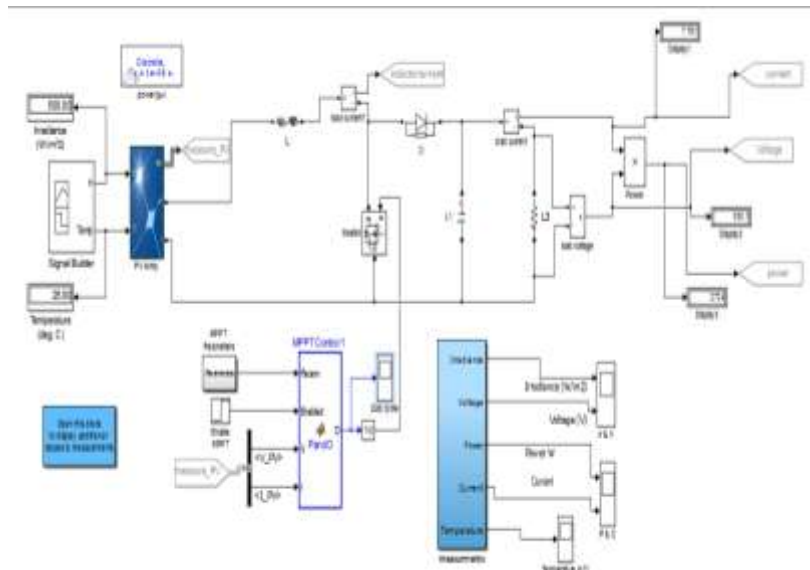


Figure 9: Circuit diagram used for the simulation of MPPT hard boost converter

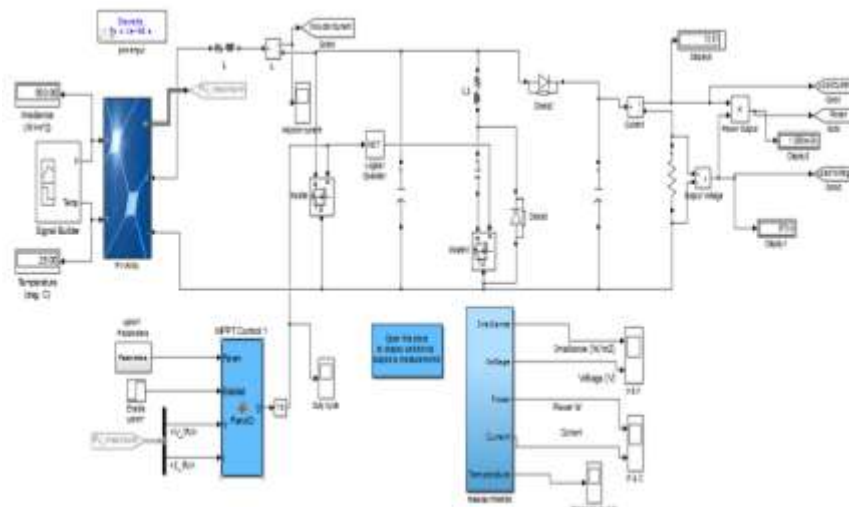


Figure 10: Circuit diagram used for the simulation of MPPT soft boost converter

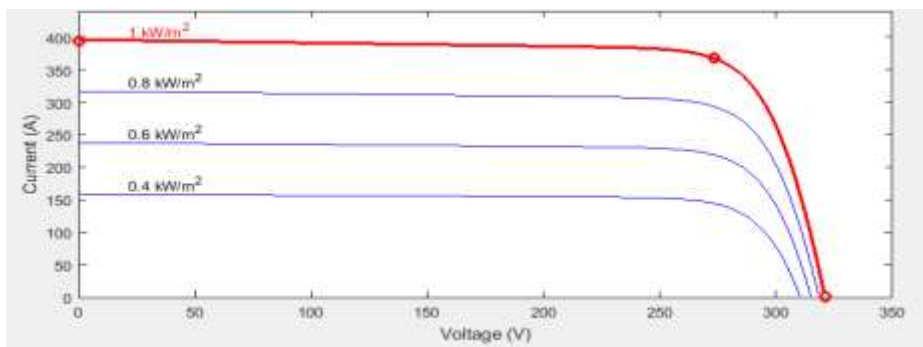


Figure 11: I-V curve (at 25°C, 1000, 800, 600 and 400W/m² respectively)

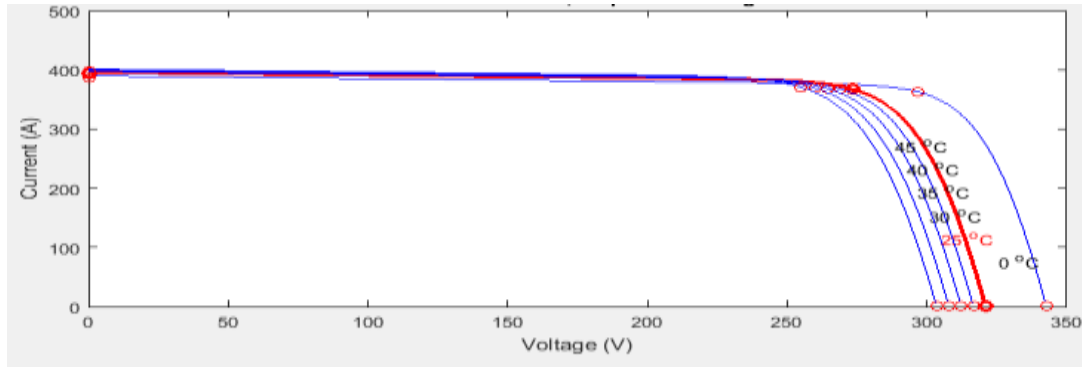


Figure 12: I-V curve at $1000\text{W}/\text{m}^2$ with varying temperatures as obtained in Matlab

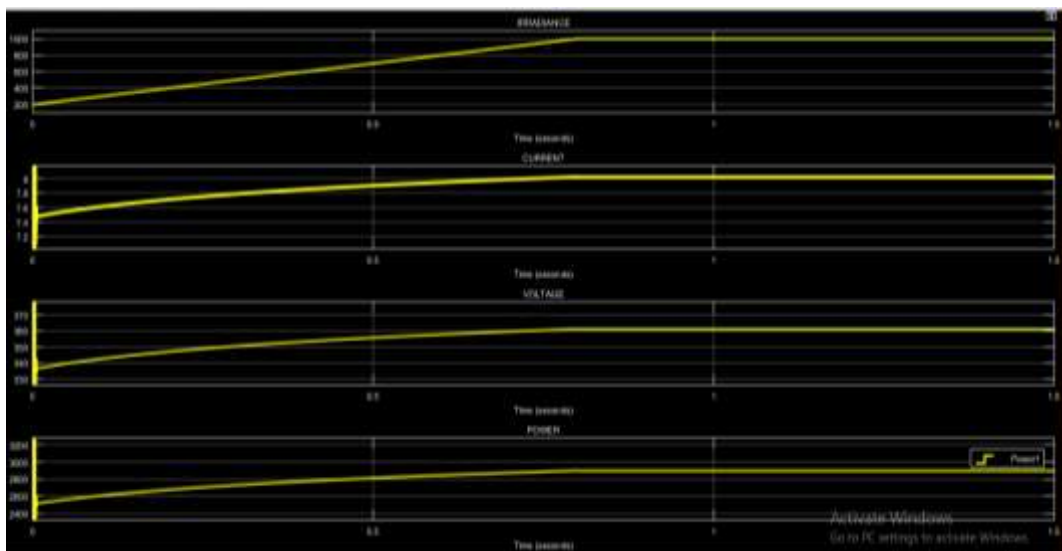


Figure 13: waveform of irradiance, output current, voltage and power of the MPPT hard boost converter at constant temperature and varying irradiances

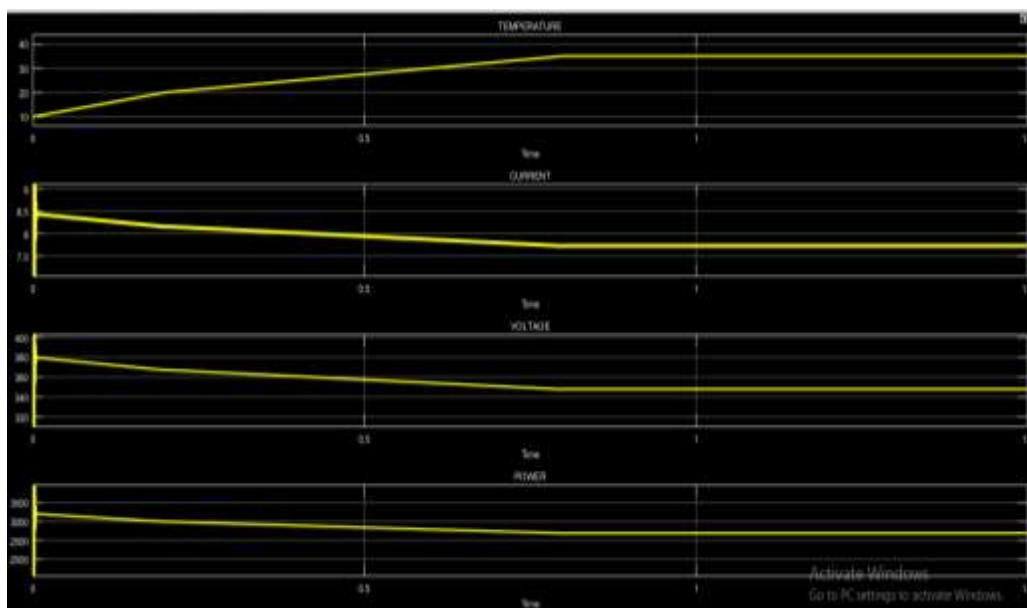


Figure 14: Waveform of temperature, output current, voltage and power of the MPPT hard boost converter at constant irradiance and varying temperature

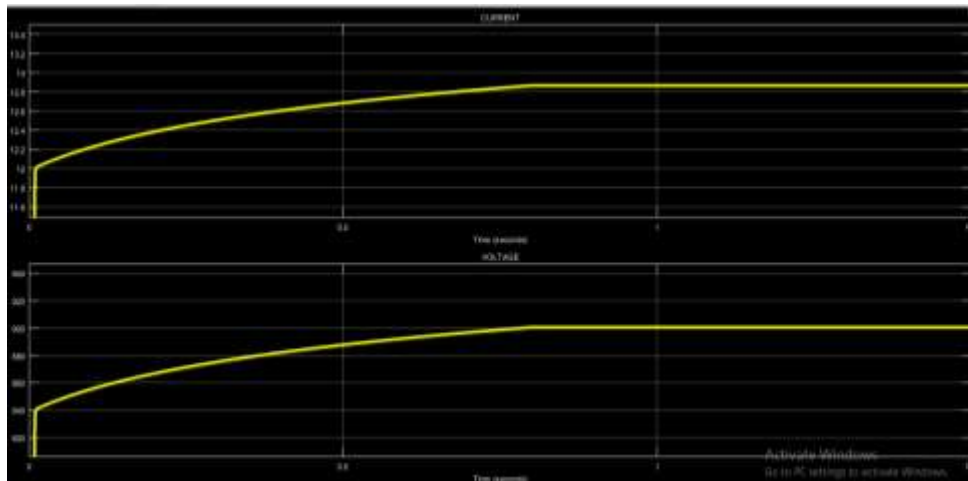


Figure 15: Waveform of output current and voltage of the MPPT soft boost converter at constant temperature and varying irradiances.

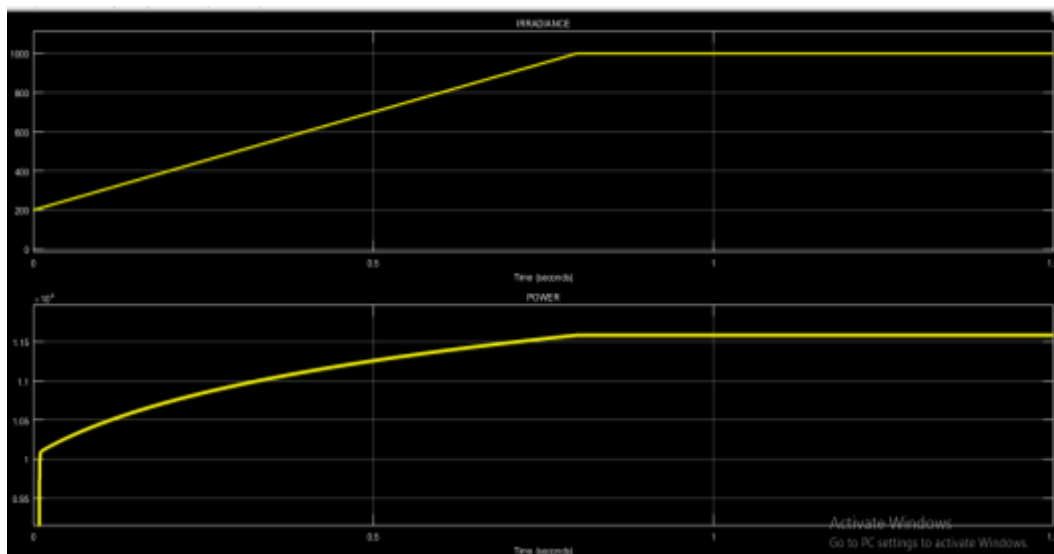


Figure 16: Waveform of Irradiance and power of the MPPT soft boost converter at constant temperature and varying irradiances.

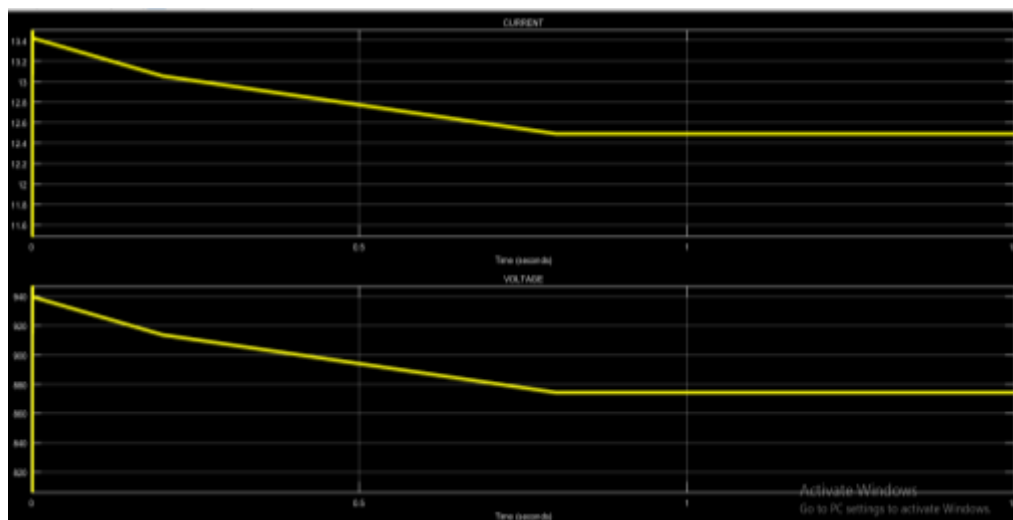


Figure 17: Waveform of output current and voltage of the MPPT soft boost converter at constant irradiances and varying temperature.

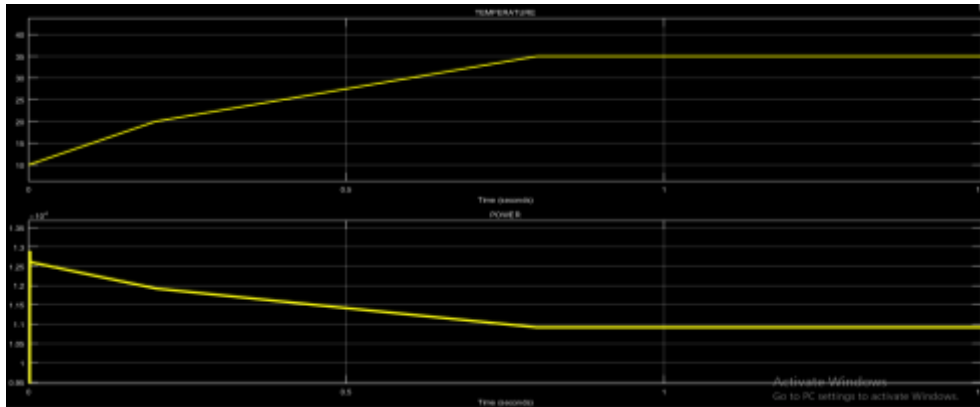


Figure 18: Waveform of temperature and power of the MPPT soft boost converter at constant Irradiance and varying temperature.

The simulation and experiments are built to evaluate the output in terms of current; voltage and power of the switching boost converter with perturb and observe algorithm and the introduced PV system at various irradiation and temperature levels. It was observed that at different irradiation and temperature levels, the PV panel current increases or decreases while the voltage shows a marginal shift. This characteristic informs us that the solar power is behaving as a current source. It also shows a rise in load power, load current and load voltage as the irradiation increases.

With MPPT there is no need to input the duty cycle, the algorithm iterates and decides the duty cycle by itself. But if an MPPT had not been interfaced to the boost converter, then there would be a need to input the duty cycle to the system. But if constant duty cycle is used, the maximum power point cannot be tracked and thus the system is less efficient.

Comparison of MPPT hard and soft switching boost converter

The tables below show the effect of varying irradiation and temperature on output of the PV system. Table 1 shows the values of output current, voltage and power of hard switching boost converter at various irradiation and temperature. (a) at constant temperature of 25°C and irradiance(W/m²) of 200, 400, 600, 800 and 1000 (b) at constant irradiance of 1000W/m² and temperature(°C) of 10, 20, 25, 30, 35 and 40

(a)

Irradiance (W/m ²)	Current(A)	Voltage(V)	Power(W)
200	14.188 × 10 ⁻³	638.482 × 10 ⁻³	9.059 × 10 ⁻³
400	7.710	346.968	2.675 × 10 ³
600	7.851	353.281	2.774 × 10 ³
800	7.949	357.694	2.843 × 10 ³
1000	8.021	360.960	2.895 × 10 ³

(b)

Temperature (°C)	Current(A)	Voltage(V)	Power(W)
10	69.815 × 10 ⁻³	3.142	219.338 × 10 ⁻³
20	8.152	366.838	2.990 × 10 ³
25	8.014	360.610	2.890 × 10 ³
30	7.868	354.056	2.786 × 10 ³
35	7.721	347.446	2.683 × 10 ³
40	7.585	341.343	2.589 × 10 ³

Table 2 shows the value of output current, voltage and power of soft switching boost converter at various irradiation and temperature. (a) at constant temperature of 25°C and irradiance(W/m²) of 100, 200, 400, 600, 800 and 1000 (b) at constant irradiance of 1000W/m² and temperature(°C) of 10, 20, 25, 30, 35 and 40

(a)

Irradiance (W/m ²)	Current(A)	Voltage(V)	Power(W)
100	664.736 × 10 ⁻⁶	46.532 × 10 ⁻³	30.931 × 10 ⁻⁶
200	11.980	638.599	10.046 × 10 ³
400	12.385	866.940	10.737 × 10 ³
600	12.602	882.156	11.117 × 10 ³
800	12.751	892.543	11.380 × 10 ³
1000	12.865	900.516	11.585 × 10 ³

(b)

Temperature (°C)	Current(A)	Voltage(V)	Power(W)
10	13.974×10^{-3}	978.176×10^{-3}	13.669×10^{-3}
20	13.052	913.614	11.924×10^3
25	12.864	900.464	11.583×10^3
30	12.677	887.379	11.249×10^3
35	12.488	874.175	10.917×10^3
40	12.301	861.052	10.592×10^3

From table 1(a), at irradiation of 600 and 1000, the hard switching boost converter generates 2.774kW and 2.895kW power respectively at a constant temperature of 25 degrees Celsius. From table 2(a), at irradiation of 600 and 1000, the soft switching boost converter generates 11.117kW and 11.585kW power respectively at a constant temperature of 25 degrees Celsius. This result clearly shows that the soft switching techniques generate higher output power than the hard switching method. This is possible because the soft switching technique reduces switching and conduction losses as a result of its auxiliary resonant circuit. Also it shows that the soft switching approach will increase the efficiency of the PV system as compared to the hard switching method.

IV. CONCLUSION

All of the analysis and calculations discussed in this work have been experimented by this MPPT boost converter design using perturb and observe techniques. Simulations using calculated parameters were performed in MATLAB Simulink and corresponding waveforms were obtained. The power efficiency of the circuit was obtained to be about 90 %. However an additional constraint needs to be put on the load. The load must not exceed 75Ω as this will cause the efficiency of the MPPT boost converter to fall below the specified value of about 90%. It was observed that when the load exceeds this critical value, the circuit operates in discontinuous conduction mode. Furthermore, it is observed that at varying duty cycle of a switching boost converter, the output voltage also changes. As can be seen from the results, the maximum power point is tracked as the irradiation changes and as irradiation increases the maximum PV panel current increases while the maximum PV panel voltage is almost constant. Also using the soft switching boost converter will greatly increase the overall efficiency of the MPPT system.

REFERENCES

- [1]. Hussein, K; Muta, I. Hoshino, T. and Osakada, M. (1995) "Maximum photovoltaic power tracking: An algorithm for rapidly changing atmospheric conditions," IEE Proceedings: Generation, Transmission and Distribution, vol. 142, no. 1, pp. 59–64.
- [2]. Kyocera, KC200GT (2013)—"High Efficiency Multicrystal Photovoltaic Module" <http://www.kyocerasolar.com/assets/001/5195.pdf>.
- [3]. Esram T. and Chapman, P. L. (2007) "Comparison of Photovoltaic Array Maximum Power Point Tracking Techniques," Energy Conversion, IEEE Transactions on, vol. 22, pp. 439-449.
- [4]. Villalva M. G. and E. Ruppert F. (2009) "Analysis and simulation of the P&O MPPT algorithm using a linearized PV array model," in Proceedings of the 35th Annual Conference of the IEEE Industrial Electronics Society (IECON '09), pp. 231–236.
- [5]. Faranda R. and Leva, S. (2008) "Energy Comparison of MPPT techniques for PV Systems," WSES Transaction on Power Systems, vol. 3, pp. 446-455.
- [6]. Salam, Z., Kashif I. and Hamed T. (2010) "An improved two-diode photovoltaic (PV) model for PV system" International Conference of the IEEE on Power Electronics, Drives and Energy Systems (PEDES) & 2010 Power India, pp. 1-5
- [7]. Vikrant.A.Chaudhari, (2005) "Automatic Peak Power Tracker for Solar PV Modules Using dSpacer Software," in Maulana Azad National Institute of Technology vol. Degree of Master of Technology In Energy. Bhopal: Deemed University, pp. 98.
- [8]. Sera, D, Kerekes, T, Teodorescu, R. and Blaabjerg, F. (2006) "Improved MPPT method for rapidly changing environmental conditions," in IEEE International Symposium on Industrial Electronics, pp. 1420-1425.
- [9]. Barakati S.M., Kazerani M., and Aplevich J.D., (2009) "Maximum Power Tracking Control for a Wind Turbine System Including a Matrix Converter". IEEE Trans. Energy Convers., 24,3, 705–713.
- [10]. Ahmad M.E. and Mekhilef, S. (2009) "Design and Implementation of a Multilevel Three-Phase Inverter with Less Switches and Low Output Voltage Distortion," Journal of Power Electronics, vol. 9, pp. 594-604.
- [11]. Xiao, W. Ozog, N. and Dunford, W. G. (2007) "Topology study of photovoltaic interface for maximum power point tracking," IEEE Transactions on Industrial Electronics, vol. 54, no. 3, pp. 1696–1704.
- [12]. Veerachary, M. Senjyu, T. and Uezato, K. (2001) "Maximum power point tracking control of IDB converter supplied PV system," Electric Power Applications, IEE Proceedings -, vol. 148, pp. 494-502.
- [13]. Park, S.H. Cha, G.R. Jung Y.C. and Won, C.Y. (2010) "Design and Application from PV Generation System Using a Soft-Switching Boost Converter with SARC", IEEE Transactions on Industrial Electronics, vol.57, no.2, pp. 515-522.

Ifeanyi B. Ezugwu "Design And Simulation Of A Maximum Power Point Tracking (Mppt) For A Boost Converter Fed From A Pv Source "American Journal of Engineering Research (AJER), vol. 7, no. 09, 2018, pp. 185-196